ACCEPTED BY ApJ
Preprint typeset using LaTeX style emulateapj v. 5/2/11

THE LARGE SCALE MAGNETIC FIELDS OF THIN ACCRETION DISKS

XINWU CAO[1] AND HENDRIK C. SPRUIT[2]
[1] Key Laboratory for Research in Galaxies and Cosmology, Shanghai Astronomical Observatory, Chinese Academy of Sciences, 80 Nandan Road, Shanghai, 200030, China; cxw@shao.ac.cn and
[2] Max Planck Institute for Astrophysics, Karl-Schwarzschild-Str. 1, 85748, Garching, Germany; henk@mpa-garching.mpg.de
accepted by ApJ

ABSTRACT

Large scale magnetic field threading an accretion disk is a key ingredient in the jet formation model. The most attractive scenario for the origin of such a large scale field is the advection of the field by the gas in the accretion disk from the interstellar medium or a companion star. However, it is realized that outward diffusion of the accreted field is fast compared to the inward accretion velocity in a geometrically thin accretion disk if the value of the Prandtl number P_m is around unity. In this work, we revisit this problem considering the angular momentum of the disk is removed predominantly by the magnetically driven outflows. The radial velocity of the disk is significantly increased due to the presence of the outflows. Using a simplified model for the vertical disk structure, we find that even moderately weak fields can cause sufficient angular momentum loss via a magnetic wind to balance outward diffusion. There are two equilibrium points, one at low field strengths corresponding to a plasma-beta at the midplane of order several hundred, and one for strong accreted fields, $\beta \sim 1$. We surmise that the first is relevant for the accretion of weak, possibly external, fields through the outer parts of the disk, while the latter one could explain the tendency, observed in full 3D numerical simulations, of strong flux bundles at the centers of disk to stay confined in spite of strong MRI turbulence surrounding them.
Subject headings: accretion, accretion disks, galaxies: jets, magnetic fields

1. INTRODUCTION

Jets/outflows are observed in different types of the sources, such as, active galactic nuclei (AGNs), X-ray binaries, and young stellar objects, which are probably driven from the accretion disk through the magnetic field lines threading the disk (see reviews in Spruit 1996; Konigl & Pudritz 2000; Pudritz et al. 2007; Spruit 2010). The large scale magnetic field co-rotates with the gases in the disk, and the jets/outflows are powered by the gravitation energy released by accretion of the gases through the ordered field threading the disk. A large scale magnetic field, of uniform polarity threading the inner parts of the disk is probably a key ingredient in this jet formation model.

The origin of such a field is not well understood, however, since the net magnetic flux threading a disk cannot be produced or changed by internal processes in the disk (a consequence of the solenoidal nature of the magnetic field, see e.g. Spruit 2010). A net magnetic flux in the inner disk must therefore either be inherited from initial conditions, or somehow be accreted from a larger distance; ultimately for example from the interstellar medium or a companion star (cf. Bisnovatyi-Kogan & Ruzmaikin 1974, 1976).

One could imagine a steady state in which the inward advection of the field lines is balanced by the outward movement of field lines due to magnetic diffusion. In conventional isotropic idealizations of a turbulent plasma, it is expected (e.g. Parker 1979) that $\nu \sim \eta \sim l v_t$, in which l is the largest eddy size, and v_t is turnover velocity, i.e. $P_m \sim 1$. Whether this is actually the case in MRI turbulence has been investigated using numerical simulations (e.g., Yousef et al. 2003; Lesur & Longaretti 2009; Fromang & Stone 2009; Guan & Gammie 2009). The results all suggest that the effective magnetic Prandtl number is around unity. Fromang et al. (2009), for example, measure $P_m \approx 2$. For such Prandtl numbers a vertical field (perpendicular to the disk plane) can indeed be dragged efficiently by an advection dominated accretion flow (Cao 2011), which is hot and geometrically thick (Narayan & Yi 1994, 1995).

The advection of the field in a geometrically thin ($H/r \ll 1$), turbulent accretion disk is inefficient, however, because the radial component of the magnetic field diffuses much faster across the disk, on a time scale $\sim H^2/\eta$. As a result, a magnetic field with inclination $B_r/B_z \sim 1$ actually diffuses outward on a time scale of order H/r shorter than a purely vertical field (van Ballegooijen 1989). An inclined field is a necessary consequence of effective accretion of the field, however, since the accumulation of field lines in the inner disk exerts a pressure that causes the field above the disk to spread outward. While such an inclined configuration is favorable for launching a flow (Blandford & Payne 1982; Cao & Spruit 1994), it raises the problem how it can be accreted effectively against the action of magnetic diffusion.

Several alternatives were suggested to resolve the difficulty of field advection in thin accretion disks. Spruit & Uzdensky (2005) suggested that a weak large-scale magnetic field threads the disk in the form of localized patches in which the field is strong enough to cause efficient angular momentum through a magnetic wind. General relativistic magnetohydrodynamic (GRMHD) simulations of an accretion torus embedded in a large-scale magnetic field showed that a central magnetic flux bundle, once formed from a suitable initial condition, can survive in spite of MRI turbulence present in the disk surrounding it (Beckwith et al. 2009). The calculations by Guilet & Ogilvie (2012a) and Guilet & Ogilvie (2012b) show that the accretion velocity of the gas in the region away from the midplane of the disk can be larger than that at the midplane of the disk, which may partially solve the problem of too efficient diffusion of the field in thin accretion disk.

The outward diffusion of the field could be balanced by accretion if a process can be found that increases the accretion velocity by a factor $\sim r/H$ relative to the rate due to the turbulence alone. We explore here the conditions under this can be

achieved by a magnetic wind generated by the weak magnetic field that is to be accreted.

2. MODEL

2.1. *Model assumptions*

Apart from the accreted field, the disk model we use is a standard α–disk model, i.e. with a viscosity ν parametrized as $\nu = \alpha c_s H$, where c_s is the (isothermal) sound speed, H is the scale height of the disk, and $\alpha \sim 0.01-0.1$ (the range of values measured in MRI simulations). The field to be accreted is assumed to be sufficiently weak that it does not suppress magnetororational instability. The disk thus contains an MRI-generated field as well as a weaker field of uniform polarity threading the disk.

Since the accretion velocity that is to be achieved exceeds the viscous rate, we simplify the analysis by assuming the accretion flow to be dominated by the angular momentum loss from the accreted field, ignoring the viscous contribution from the MRI turbulence. The resulting accretion rate then has to exceed outward diffusion due to the MRI turbulence. The turbulence is assumed to produce an effective magnetic diffusivity corresponding to a magnetic Prandtl number $\mathrm{P_m} \sim 1$.

The model needs a prescription for the angular momentum loss produced by the accreting weak magnetic field. For this we use the Weber-Davis model for a magnetically driven wind, in the 'cold' approximation (in which the gas pressure force is neglected). It leads to a simple description in terms of the field strength and mass loss rate (Mestel 2012, Spruit 1996). The Weber-Davis model strictly applies only to the 'split monopole' configuration, in which the poloidal field is purely radial. Its properties are found to be a rather good approximation for more general poloidal field shapes as well (Anderson et al. 2005), which makes it adequate for the present purpose.

The angular momentum loss in this model can be characterized by a single dimensionless constant, a 'mass load parameter' μ (c.f. Michel 1969, Mestel, 2012):

$$\mu = \chi 4\pi\Omega r_0/B_\mathrm{p}, \tag{1}$$

where $B_\mathrm{p} = (B_z^2 + B_r^2)^{1/2}$ is the poloidal component of the accreted field at radius r_0 on the surface of the disk, and Ω the rotation rate at r_0 (cylindrical coordinates r, ϕ, z). χ is a constant along the flow, it is a measure of the 'mass flux per field line':

$$\chi = \rho v_\mathrm{p}/B_\mathrm{p}, \tag{2}$$

where ρ, v_p, B_p are the mass density, poloidal velocity and poloidal field strength. It is related to the mass flux per unit surface area from the disk $\dot{m}_\mathrm{w}$ by

$$\dot{m}_\mathrm{w} = B_z\chi. \tag{3}$$

The asymptotic velocity of the wind decreases monotonically with increasing μ, and for $\mu = 1$ equals the rotation velocity at r_0. The angular momentum loss increases monotonically with μ.

It turns out that the conditions for effective accretion of the field can be satisfied when $\mu \gtrsim \alpha\,\mathrm{P_m}\,r/H$. This is described in the following sections, using a specific model for the disk structure.

2.2. *The magnetic field of the disk*

The angular momentum equation for a steady accretion disk with outflows is

$$\frac{d}{dr}(2\pi r\Sigma v_r r^2\Omega) = \frac{d}{dr}(2\pi r\nu\Sigma r^2\frac{d\Omega}{dr}) - 2\pi r T_\mathrm{m}, \tag{4}$$

where Σ is the total surface mass density of the disk (counting both sides), T_m the total torque per unit of surface area of the disk (counting both sides) due to the magnetically driven outflows. Integrating Eq. (4), yields

$$2\pi r\Sigma v_r r^2\Omega = 2\pi r\nu\Sigma r^2\frac{d\Omega}{dr} - 2\pi f_\mathrm{m}(r) + C, \tag{5}$$

where the value of the integral constant C can be determined with a boundary condition on the accreting object, and

$$rT_\mathrm{m} = \frac{d f_\mathrm{m}(r)}{dr}. \tag{6}$$

The magnetic torque in unit surface disk area exerted by the outflows is

$$T_\mathrm{m} = 2\dot{m}_\mathrm{w} r_\mathrm{A}^2\Omega, \tag{7}$$

where $\dot{m}_\mathrm{w}$ is the mass loss rate in the outflow from a unit surface area of the disk (single sided), r_A is the (cylindrical) Alfvén radius of the outflow, $\Omega(r)$ is the angular velocity of the disk, and r is the radius of the field line foot point at the disk surface. The dimensionless mass load parameter μ of the outflow is

$$\mu = \frac{4\pi\rho_\mathrm{w} v_\mathrm{w}\Omega r}{B_\mathrm{p}^2} = \frac{4\pi\Omega r}{B_\mathrm{p}B_z}\dot{m}_\mathrm{w}, \tag{8}$$

where $\rho_\mathrm{w} v_\mathrm{w} = \dot{m}_\mathrm{w} B_\mathrm{p}/B_z$ is the mass flux parallel to the field line. In the cold Weber-Davis model the Alfvén radius is

$$r_\mathrm{A} = r\left[\frac{3}{2}(1+\mu^{-2/3})\right]^{1/2}. \tag{9}$$

[For more detailed discussion of this model see Mestel (2012) or Spruit (1996)]. MHD simulations of axisymmetric magnetically driven flows have shown that relations like (9) and (10) below are fair approximations for more general configurations than the Weber-Davis 'split monopole' (cf. Fig. 7 in Anderson et al. 2005). Substituting Eqs. (9) and (8) into (7), we find

$$T_\mathrm{m} = \frac{3}{4\pi} r B_\mathrm{p}^2\mu(1+\mu^{-2/3}). \tag{10}$$

The radial velocity of an accretion flow in which the angular momentum is removed predominantly by the outflows can be estimated from Eq. (4):

$$v_r \sim -\frac{T_\mathrm{m}}{\Sigma}\left[\frac{d}{dr}(r^2\Omega)\right]^{-1} \simeq -\frac{2T_\mathrm{m}}{\Sigma r\Omega}, \tag{11}$$

where we have assumed that the rotation is approximately Keplerian, $\Omega \approx \Omega_\mathrm{K}$. [This is sufficient for the following estimates, but has to be made more precise when considering the wind launching conditions (section 2.3).] The mass accretion rate of the accretion disk is

$$\dot{M} = -2\pi r\Sigma v_r \simeq \frac{4\pi T_\mathrm{m}}{\Omega}, \tag{12}$$

where Eq. (11) is used. We can compare the mass loss rate in the outflows with the accretion rate through the disk. Using (8), (10) and (12):

$$\frac{d\ln\dot{M}}{d\ln r} = \frac{4\pi r^2\dot{m}_\mathrm{w}}{\dot{M}} = \frac{1}{3}(1+\mu^{-2/3})^{-1}. \tag{13}$$

This shows that for large mass loading parameters, $\mu \gtrsim 1$, a fraction $\sim 1/3$ of the accretion rate can be lost in the wind, if the wind is sustained across the disk over a distance of order r. For $\mu \lesssim 1$ the mass loss in the wind is not significant compared with the accretion rate. Substituting (10) into (11), we obtain

$$v_r = -\frac{6c_s g(\mu)}{\Omega H \beta_p} c_s, \tag{14}$$

where $g = \mu(1+\mu^{-2/3})$, c_s is the sound speed of the gas in the midplane of the disk, and

$$\beta_p = p_c / \frac{B_p^2}{8\pi} \tag{15}$$

is a measure of the poloidal field strength at the surface relative to p_c, the gas pressure at the midplane of the disk. The magnetic field is advected inwards on a timescale

$$\tau_{adv} \sim \frac{r}{|v_r|} = \frac{r}{c_s} \frac{\Omega H \beta_p}{6 c_s g(\mu)}. \tag{16}$$

In the limit $H/r \ll 1$, the radial component of the field dominates the outward diffusion timescale τ_{diff} of the magnetic field (van Ballegooijen 1989, Lubow et al. 1994). Let

$$\kappa_0 = B_z / B_{r,s} \tag{17}$$

be the inclination, with respect to the horizontal, of the accreted field at the disk surface (s). The diffusion time scale is then of order

$$\tau_{dif} \sim \frac{rH\kappa_0}{\eta}, \tag{18}$$

where η is the magnetic diffusivity. [This dependence holds as long as $1/\kappa_0 > H/r$; in the opposite case of a nearly vertical field $B_r/B_0 < H/r$, the diffusion time is of order r^2/η]. The magnetic Prandtl number is defined as $P_m = \eta/\nu$, where ν is the turbulent viscosity. With the conventional α-parametrization, $\nu = \alpha c_s H$ we can then write Eq. (18) as

$$\tau_{dif} \sim \frac{r\kappa_0}{c_s} \frac{1}{\alpha P_m}. \tag{19}$$

For a steady state, the advection of the field in the disk has to balance the diffusion, i.e. $\tau_{adv} = \tau_{dif}$. With (16), (19) this yields a condition on the mass flux parameter μ:

$$\mu(1+\mu^{-2/3}) = \frac{\alpha \Omega H \beta_p P_m}{6 c_s \kappa_0}, \tag{20}$$

which reduces to

$$\mu(1+\mu^{-2/3}) = \frac{\alpha \beta_p P_m}{6\kappa_0} \tag{21}$$

in weak field approximation, $c_s = \Omega H$. If a significant mass flux, $\mu \sim 1$ can be launched, and assuming $\alpha = 0.01$, $P_m = 1$, and a field inclination of 30° to the vertical, this shows that a weak field with $\beta \sim 10^3$ can still be accreted through the angular momentum loss of the wind associated with it. In the following sections we investigate this with specific models for the structure of the disk.

2.3. *The mass flux in the wind*

The mass loss rate in the outflow is governed by the gas density at the position of the sonic point (in the following labeled with index $_s$), where the flow speed equals the sound speed (more accurately, the slow mode cusp speed). The mass flux, parallel to the field, is thus approximately $\rho c_{s,s}$, and per unit of surface area parallel to the disk surface, the mass flux is

$$\dot{m}_w \sim \frac{B_z}{B_p} \rho c_{s,s}\ , \tag{22}$$

where $B_p = (B_z^2 + B_r^2)^{1/2}$ as before. As mentioned, we consider only the wind associated with the accreted field. The MRI turbulence also produces a field, but being a local process, we assume that it does not produce a large scale field that would be significant for wind-driven angular momentum loss.

The mass flux depends sensitively on the surface temperature T_s. Assume a radiative disk, i.e. the vertical energy transport through the disk is by radiation. In the diffusion approximation, the surface temperature is then related to the temperature T_c of the disk at the midplane of the disk by

$$\frac{4\sigma T_c^4}{3\tau} = \sigma T_s^4, \tag{23}$$

where τ is the optical depth of the disk in the vertical direction. In terms of the sound speeds $c_{s,s}$, $c_{s,c}$ at the surface and the midplane,

$$c_{s,s} = \left(\frac{4}{3\tau}\right)^{1/8} c_{s,c}\ . \tag{24}$$

Along a field line that corotates with its footpoint in the disk the outflow is governed by an effective potential Ψ_{eff},

$$\Psi_{eff}(r,z) = \frac{GM}{(r^2+z^2)^{1/2}} - \frac{1}{2}\Omega^2 r^2, \tag{25}$$

where Ω is the angular velocity of the footpoint at the disk surface. In this expression and in the following, the (small) difference between the rotation rate Ω of the field line and the Keplerian value Ω_K has to be included consistently, since it has a strong effect on the launching conditions for the wind, through its effect on Ψ_{eff} (Ogilvie and Livio, 2001). This difference, due to the magnetic stress exerted at the surfaces follows from the radial equation of motion,

$$r\Omega_K^2 - r\Omega^2 = \frac{B_{r,s} B_z}{2\pi\Sigma} = \frac{B_z^2}{2\pi\Sigma\kappa_0}, \tag{26}$$

where Σ the total (two-sided) surface density $\Sigma \approx 2\rho_c H$. This yields

$$\Omega = \Omega_K \left[1 - \frac{2r}{\beta_z \kappa_0 H} \frac{c_s^2}{r^2\Omega_K^2}\right]^{1/2}, \tag{27}$$

which can be approximated as

$$\Omega = \Omega_K \left[1 - \frac{H}{r} \frac{2}{\beta_z \kappa_0}\right]^{1/2}, \tag{28}$$

in weak field case, where $\beta_z = 8\pi p_c / B_z^2 = \beta_p(1+\kappa_0^2)/\kappa_0^2$ is the plasma-beta of the accreted field evaluated at the midplane ($_c$) of the disk.

Next, we make the model more specific and simplify it a bit by approximating the sound speed in the launching region as constant with height. In addition we take the midplane temperature as representative for the interior of the disk. This is sufficient for the evaluation of quantities like the rotation rate correction in (28).

The location of the sonic point is close to the maximum of the effective potential. The mass flux is determined by the

density at the sonic point; a fair approximation for this is to treat the subsonic region as if it were in hydrostatic equilibrium. This yields the following estimate for the mass loss rate in an isothermal outflow (per unit of disk surface area),

$$\dot{m}_{\rm w} \sim \frac{\kappa_0}{(1+\kappa_0^2)^{1/2}} \rho_0 c_{\rm s,s} \exp\left[-(\Psi_{\rm eff,s}-\Psi_{\rm eff,0})/c_{\rm s,s}^2\right], \quad (29)$$

where ρ_0 is the density of the gas in the base of the outflow (still to be specified), and $\Psi_{\rm eff,s}$ and $\Psi_{\rm eff,0}$ are the effective potential at the sonic point and the footpoint at the disk surface, respectively. The factor involving κ_0 is equal to the ratio $B_z/B_{r,\rm s}$ in Eq. (17).

The vertical structure of an isothermal disk can be calculated with the vertical momentum equation,

$$c_{\rm s}^2 \frac{{\rm d}\rho(z)}{{\rm d}z} = -\rho(z)\Omega_{\rm K}^2 z - \frac{B_r(z)}{4\pi}\frac{{\rm d}B_r(z)}{{\rm d}z}. \quad (30)$$

In principle, the field line shape is computable by solving the radial and vertical momentum equations with suitable boundary conditions (for a detailed discussion see Cao & Spruit 2002, hereafter CS02). For the isothermal case, an approximate analytical expression is proposed for the shape of the field lines in the flow:

$$r - r_{\rm i} = \frac{H}{\kappa_0 \eta_{\rm i}^2}(1-\eta_{\rm i}^2+\eta_{\rm i}^2 z^2 H^{-2})^{1/2} - \frac{H}{\kappa_0\eta_{\rm i}^2}(1-\eta_{\rm i}^2)^{1/2}, \quad (31)$$

where $r_{\rm i}$ is the radius of the field line footpoint at the midplane of the disk, and $\eta_{\rm i} = \tanh(1)$ (see CS02). This expression reproduces the basic features of the Kippenhahn-Schlüter model for a sheet of gas suspended against gravity by a magnetic field (Kippenhahn & Schlüter 1957), for weak as well as strong field cases. As done in CS02, we use a fitting formula to calculate the scale height of the disk in the rest of this work,

$$\frac{H}{r} = \frac{1}{2}\left(\frac{4c_{\rm s,c}^2}{r^2\Omega_{\rm K}^2} + f^2\right)^{1/2} - \frac{1}{2}f, \quad (32)$$

where

$$f = \frac{1}{2(1-{\rm e}^{-1/2})\kappa_0}\frac{B_z^2}{4\pi\rho r H \Omega_{\rm K}^2 \kappa_0}. \quad (33)$$

Solving for H:

$$H = \frac{c_{\rm s,c}}{\Omega_{\rm K}}\left[1 - \frac{1}{(1-{\rm e}^{-1/2})\beta_{\rm p}(1+\kappa_0^2)}\right]^{1/2}, \quad (34)$$

which requires

$$\beta_{\rm p} > \beta_{\rm p,min} = \frac{1}{(1-{\rm e}^{-1/2})(1+\kappa_0^2)}, \quad (35)$$

or

$$\beta_{\rm z} > \beta_{\rm z,min} = \frac{1}{(1-{\rm e}^{-1/2})\kappa_0^2}. \quad (36)$$

The square bracket in (34) gives the magnetic correction to the standard relation between disk thickness and the sound speed at the midplane. It reduces to unity for a weak field, or when the radial component is small compared with the vertical component. For a typical value of $\kappa_0 \sim 1$, we find $\beta_{\rm p}$ must be $\gtrsim 1.3$. This means that the magnetic pressure can be larger than the gas pressure in the disk only if the inclination of the field line at the disk surface κ_0 is larger than unity.

Equation (32) should be a good approximation for the present investigation, especially in the thin outer region of the disk which is probably the most critical region for the accretion of a net magnetic flux. Substituting (29) into (8), the mass flow parameter is

$$\mu = \frac{4\pi\Omega r \rho_0 c_{\rm s,s}}{B_{\rm p}^2}\exp\left[-(\Psi_{\rm eff,s}-\Psi_{\rm eff,0})/c_{\rm s,s}^2\right]. \quad (37)$$

To estimate the density ρ_0 at the base of the flow, we note that Eq. (37) is applicable only at heights in the atmosphere where the field is strong enough, relative to the plasma, to enforce corotation so the effective potential Ψ is relevant for the launching process of the wind. Inside the disk, where $\beta > 1$, this is not the case. As base of the flow, where the pressure is p_0, we assume the height where the plasma-beta is of order unity, i.e.

$$\beta_{\rm s} \equiv 8\pi p_0/B_{\rm p}^2 \approx 1, \quad (38)$$

which determines p_0 if $\beta_{\rm s}$ is given. For most of calculations reported below, $\beta_{\rm s} = 1$ is used, some with a lower value 0.1. The mass flux is then related to the poloidal field strength at the disk surface by

$$\rho_0 c_{\rm s,s} = \frac{B_{\rm p}^2}{8\pi c_{\rm s,s}}. \quad (39)$$

Using (24) Eq. (37) can then be written as

$$\mu = \frac{\Omega r}{2c_{\rm s,c}}(3\tau/4)^{1/8}\exp\left[-(\Psi_{\rm eff,s}-\Psi_{\rm eff,0})/c_{\rm s,s}^2\right]. \quad (40)$$

The factor in front of the exponential tends to be a large number, the exponential itself a small one. To evaluate the effective potential as a function of height, field line inclination, and the (slightly non-Keplerian) rotation rate Ω, the model of CS02 is used. It is also used for the optical depth connecting the surface temperature to the disk midplane temperature.

3. RESULTS

The disk is compressed in the vertical direction by the curved magnetic field line, which sets an upper limit on the magnetic field strength. We plot the corresponding minimal $\beta_{\rm z}$ as a function of the field inclination κ_0 at the disk surface in Fig. 1. The curved field line also exerts a radial force on the disk against the gravity of the central object, which provides an additional constraint on the field strength (Fig. 1 show the result for different values of the disk temperature). The angular velocity Ω deviates from the Keplerian value due to the radial magnetic force. Fig. 2 shows the dimensionless angular velocity $\Omega/\Omega_{\rm K}$ of the disk as a function of κ_0 and $\Theta = c_{\rm s,c}^2/(r^2\Omega_{\rm K}^2)$.

For given values of the disk parameters, i.e., the viscosity α, the temperature parameter Θ in the disk, and the optical depth τ, the dependence of mass loading μ on $\beta_{\rm z}$ can be calculated with Eqs. (20) and (40) respectively. These relations are plotted in Figs. 3-5 for disk-outflow systems with different values of the parameters. In all calculations, $P_{\rm m} = 1$ is adopted. It is found that two branches of solutions usually exist for most cases. We plot the solutions of the disk-outflow systems in Figs. 6 and 7. The solutions with different values of $\beta_{\rm s}$ ($\beta_{\rm s} = 8\pi p_0/B_{\rm p}^2$) at the base of the outflow for the isothermal disk are compared in Figs. 8 and 9. The two branches of solutions correspond to low mass ($\mu \ll 1$) loaded outflows with strong field strength (low-β), or high mass loaded outflows

with relative weak field strength. The optical depth needed to connect surface and internal temperature has been computed by including a Rosseland mean opacity and electron scattering; it is shown in Fig. 10.

For comparison, we have repeated the calculations for a uniformly isothermal disk, that is, the temperatures of disk and wind are assumed to be the same (Figs. 8 and 9). Though this is not very realistic, it gives an impression of the sensitivity of the results to the model assumptions made.

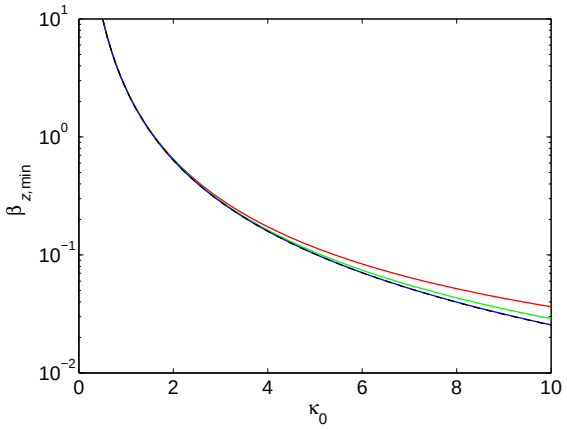

FIG. 1.— Constraints on the poloidal magnetic field strength in terms of β_z (the plasma-beta of the accreted field measured at the midplane of the disk, see text). Black line: $\beta_{z,\min}$ as constrained by the vertical pressure exerted by the curved field line (Eq. 36). Colors: the minimal values of β_p constrained by the radial magnetic force (see Eq. 27) for different disk temperatures, Θ = 0.01 (red), 2.5×10^{-4} (green), and 10^{-4} (blue).

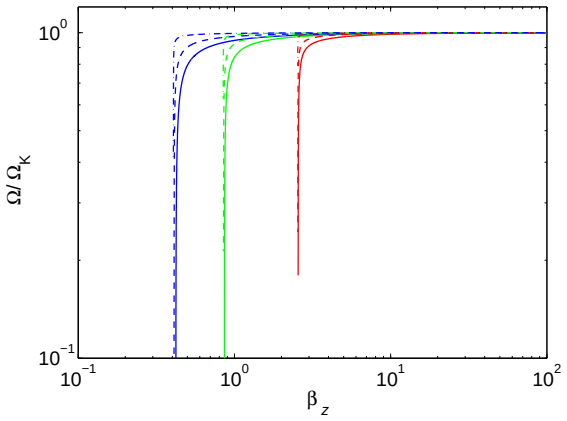

FIG. 2.— Deviation of the angular velocity of the disk Ω relative to Keplerian due to magnetic stress, as a function of β_z (Eq. 27). Field line inclination κ_0 = 1 (red), $\sqrt{3}$ (green), and 2.5 (blue). Disk temperature parameter Θ = 0.01 (solid), 2.5×10^{-4} (dashed), and 10^{-4} (dash-dotted).

3.1. *Discussion*

The magnetic field is dragged inwards by the accretion disk, an outflow is launched by this field, and the radial velocity of the accretion disk is determined by the rate of angular momentum carried away by the outflows. This loss rate in the outflows can be estimated by exploring the launching process of the outflow, which depends sensitively on the field strength/configuration and the density/temperature of the gas at the disk surface. We have used the cold Weber-Davis model for determining the mass load parameter μ of the outflow as a function of strength of the accreted field and parameters of the disk structure: its optical depth (a radiative disk is assumed), a temperature-parameter Θ, the α-viscosity, and the magnetic Prandtl number P_m of the assumed MRI turbulence (cf. Eq. 20). Balancing the resulting accretion velocity with the outward diffusion by magnetic turbulence determines the conditions for existence of a stationary disk-outflow system. Figs. 3-5 illustrate the properties of the solutions. It is found that two solution branches exist for all cases. The lower branch corresponds to high field strength and low μ, i.e., low mass loss rate, the upper one corresponds to low field strength and high μ, i.e. high mass loss rate (see Figs. 6 and 7). There is an upper limit on the field inclination κ_0 at the disk surface, which increases with disk temperature. Overcoming the deeper effective potential barrier associated with a larger inclination requires a higher internal energy of the gas. The maximum inclination κ_0 thus decreases with increasing optical depth τ of the disk, as the surface temperature decreases with increasing τ, (keeping other disk parameters fixed, see Eq. 24).

We have also explored the sensitivity to model assumptions somewhat with solutions for a more drastically simplified case, where the temperature is assumed uniform throughout, i.e. the temperature of the outflow is the same as the disk temperature. This is shown in Figs. 8 and 9. These also show the effect of assuming a lower density of the gas at the base of the outflow (β_s = 0.1). The results are qualitatively similar to those with β_s = 1.

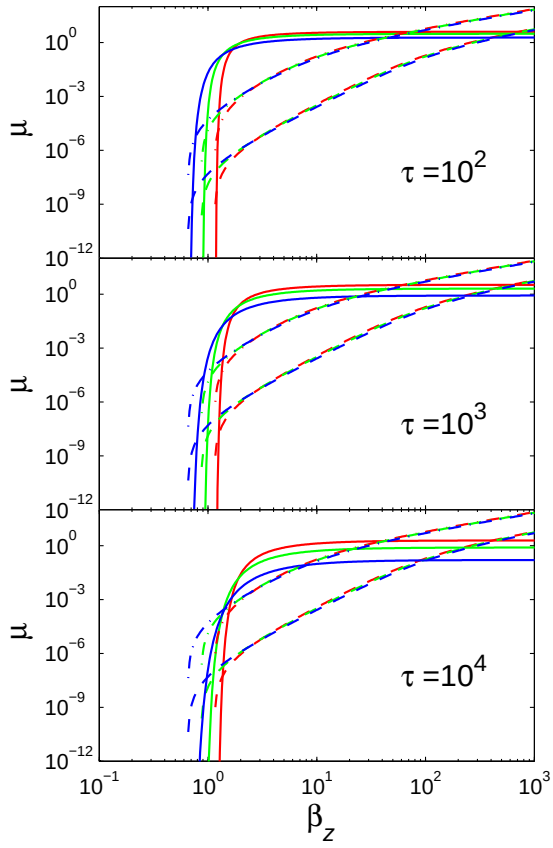

FIG. 3.— Mass loading μ as a function of β_z. Solid: as determined from the wind launching conditions Eq. (40). Broken: mass loading required for effective accretion of the field lines (20), for disk viscosity $\alpha = 0.1$ (dashed)) and $\alpha = 1$ (dash-dotted). The intersection points are possible solutions for the stationary wind driven accretion problem. Field line inclinations are $\kappa_0 = 1.5$ (red), $\sqrt{3}$ (green), and 2 (blue). The disk temperature parameter $\Theta = 0.01$, magnetic Prandtl number $P_m = 1$.

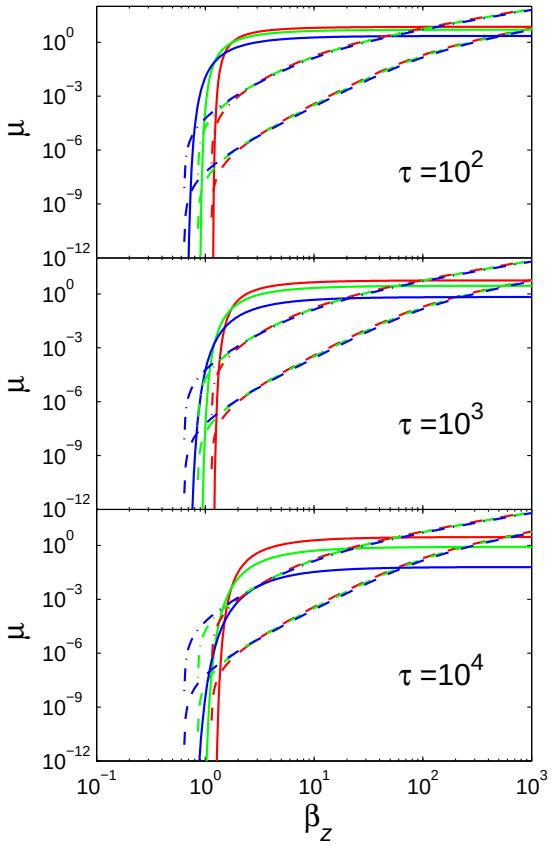

FIG. 4.— As Fig. 3 for $\Theta = 2.5 \times 10^{-4}$.

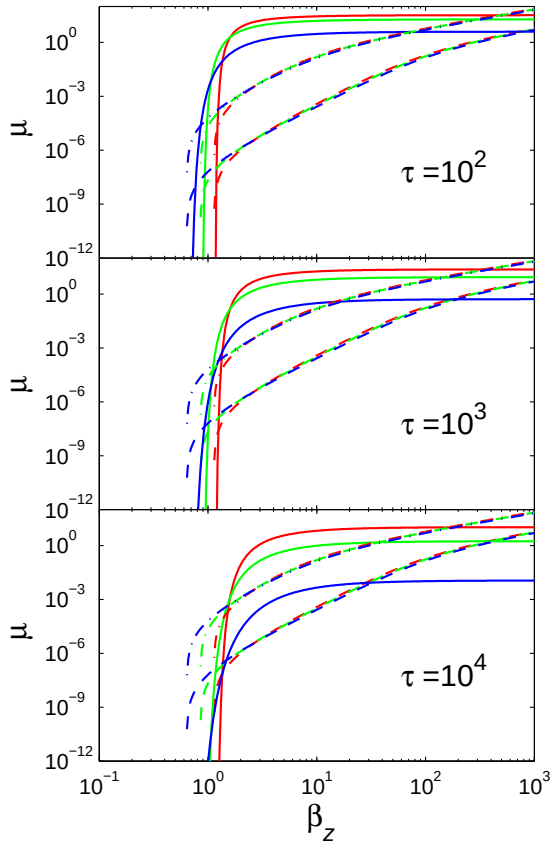

FIG. 5.— As Fig. 3, for $\Theta = 10^{-4}$.

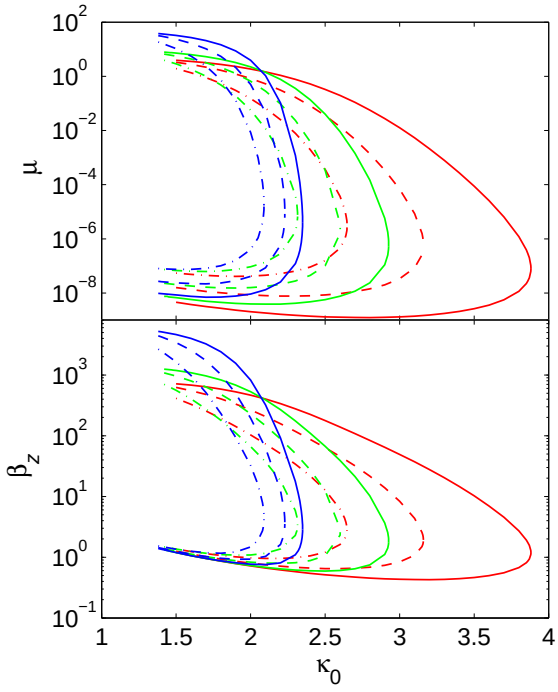

FIG. 6.— Resulting disk-outflow solutions for different disk temperature parameters: $\Theta = 0.01$ (red), 2.5×10^{-4} (green), and 10^{-4} (blue), and different values of the disk optical depth: $\tau = 10^2$ (solid), 10^3 (dashed), and 10^4 (dash-dotted). The viscosity parameter $\alpha = 0.1$.

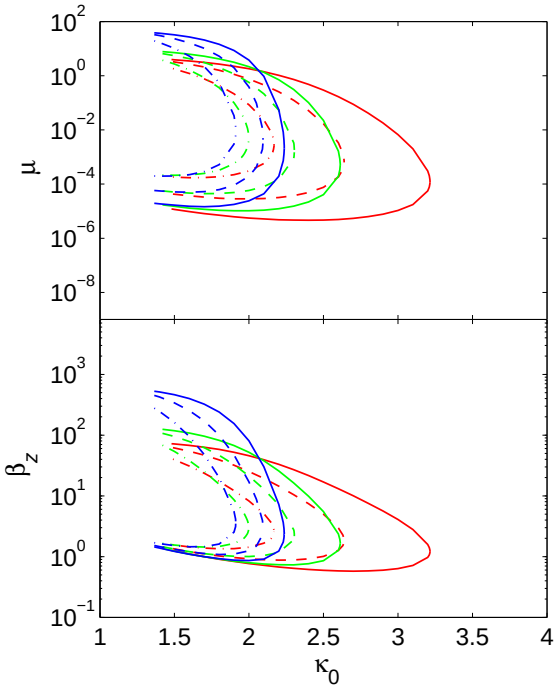

FIG. 7.— As Fig. 6, for $\alpha = 1$.

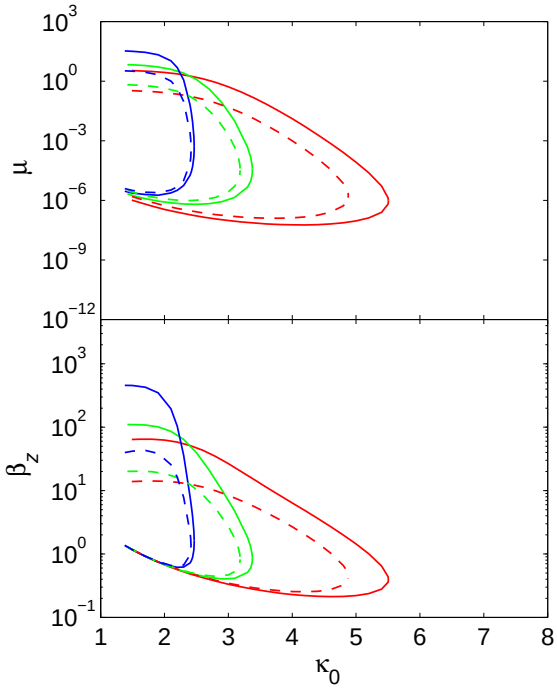

FIG. 9.— The same as Fig. 8, for $\alpha = 1$.

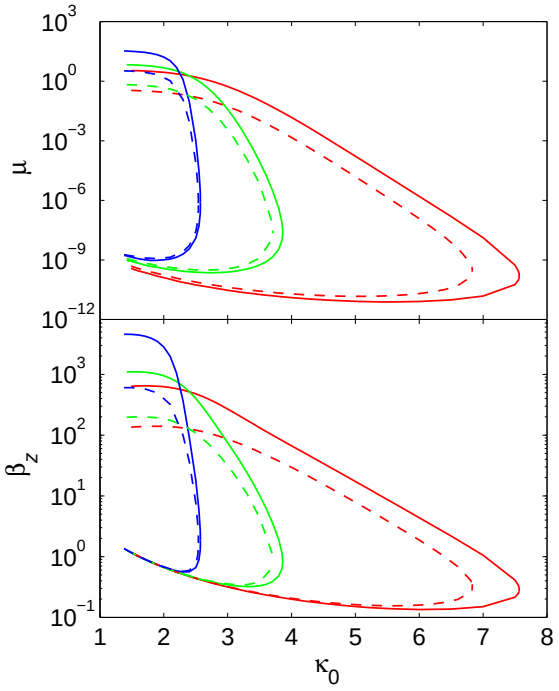

FIG. 8.— The disk-outflow solutions for vertically isothermal accretion disks. The colored lines represent the solutions derived with different disk temperature, $\Theta = 0.01$ (red), 2.5×10^{-4} (green), and 10^{-4} (blue), respectively. The solutions derived with different ratios of gas pressure to magnetic pressure at the disk surface are indicated with different line types, $\beta_s = 1$ (solid), and 0.1 (dashed), respectively. Viscosity parameter $\alpha = 0.1$.

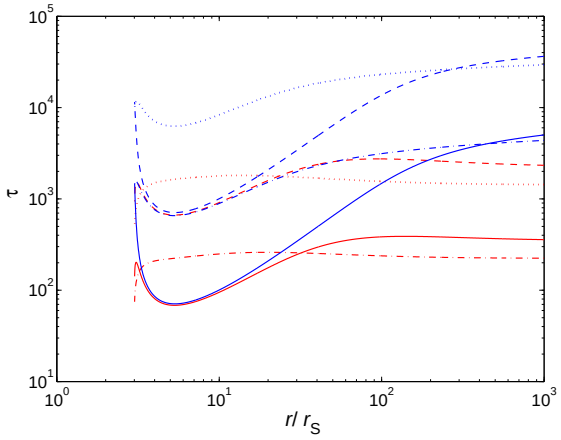

FIG. 10.— The optical depth of the standard thin accretion disks without magnetic field as functions of radius, where $r_S = 2GM/c^2$. The opacity $\kappa_{tot} = \kappa_{es} + \kappa_R$ is adopted, where the Rosseland mean opacity $\kappa_R = 5 \times 10^{24} \rho T_c^{-7/2}$ cm^2 g^{-1}. The red lines represent the results calculated for a black hole with $M = 10 M_\odot$, while the blue lines are for a black hole with $M = 10^8 M_\odot$. The different line types correspond to the disks with different parameters: solid ($\alpha = 1$ and $\dot{m} = 0.1$), dashed ($\alpha = 0.1$ and $\dot{m} = 0.1$), dash-dotted ($\alpha = 1$ and $\dot{m} = 0.01$), and dotted lines ($\alpha = 0.1$ and $\dot{m} = 0.01$).

The dependence of the solutions on the value of α is shown in Fig. 7. The magnetic diffusivity η is scaled with the turbulent viscosity ν, and therefore the diffusion becomes more important for the cases with a higher value of the viscosity parameter α. In order to compete with the diffusion of the field, a large radial velocity of the disk is required for high α cases, which corresponds a high rate of angular momentum removal by the outflows. We find that the values of the mass load parameter μ of the outflow are systematically higher for those derived with a larger α (compare the results in Figs. 6 and 7).

The accretion disk is vertically compressed by the curved magnetic field, which sets an upper limit on the field strength (see Eqs. 35 and 36). The value of $\beta_{z,\min}$ only depends on the field inclination κ_0 at the disk surface, and $\beta_{z,\min}$ decreases with increasing κ_0 (see Fig. 1). There is a force exerted on the disk by the curved field against the gravity of the central object in the radial direction, which makes the rotation of the gas in the disk be sub-Keplerian. The rotational velocity of the disk can be quite low if the field strength is sufficiently strong (see Eq. 27 and Fig. 2). The disk is then magnetically supported against gravity. Such configurations are likely to be unstable to interchange instabilities, however (Spruit et al. 1995), which effectively cause the magnetic field to spread outward and limit the field strength (as observed in the numerical simulations of Stehle & Spruit 2001). The requirement that the magnetic force is less than the gravity in the radial direction provides an additional constraint on the field strength. We find that the constraints almost overlap with that constrained by the force in the vertical direction when $\kappa_0 \lesssim 3$, while maximal field strength becomes lower (a larger $\beta_{\min}$) for a disk with relative high temperature and $\kappa_0 \gtrsim 3$ (see Fig. 1).

From Fig. 1 we see that the magnetic field can be very strong, e.g., the magnetic pressure can be more than one order of magnitude higher than the gas pressure in the disk if the field inclination κ_0 is sufficiently large. However, the magnetically driven outflow will be suppressed if κ_0 is too large, because the effective potential barrier becomes extremely deep in this case. The results show that $\beta \gtrsim 0.5$ is always satisfied in the disk-outflow solutions (see Figs. 6 and 7). Note that this does not mean the magnetic field cannot be strong, as the disk is significantly compressed in the vertical direction, which increases the density of the disk and then the gas pressure for given disk temperature.

3.2. *Stability*

We have calculated only stationary solutions, but their stability to time-dependent perturbations can already be guessed at by inspection of the intersection points in Fig. 3. Near the high-beta (low field) solution the mass loading parameter (solid line) is nearly independent of the field strength assumed (this is because of the assumed value of the plasma-beta at the base of the flow). If the field strength were to decrease (to the right of the intersection point), the mass loss would need to increase in order to maintain a balance between inward accretion and outward diffusion (dashed line). Since the mass loading actually does not change much, the angular momentum loss is insufficient to balance outward diffusion for such a perturbation. Outward diffusion will then tend to decrease the field strength, providing a positive feedback to the perturbation. This stationary solution is thus expected to be unstable.

This mechanism of instability is the same as that identified in the linear stability analysis of CS02. The timescale of the instability is comparable with the dynamical timescale of the disk if the magnetic torque is large, which becomes significantly small when the magnetic torque is weak (see CS02 for the detailed results and discussion). At sufficiently low field strengths or/and high-κ_0, where the magnetic torque becomes weak, this analysis predicted a regime of stability due to magnetic diffusion. This implies that the growth timescale of such instability considered in this work should be significantly lower than the dynamical timescale of the disk. The detailed calculation of the instability is beyond the scope of this work.

New is the high-field solution found (leftmost intersection). By the same line of reasoning as above, this point is expected to be stable, since the slopes of the dashed and solid curves are reversed here. It is, however, somewhat outside the assumptions made, since the MRI turbulence that was assumed for the magnetic diffusion is probably suppressed at these field strengths. Instead, instability of the strong field itself is likely to cause its outward diffusion (as in the simulations of Stehle & Spruit 2001 and Igumenschev et al. 2003). To the (uncertain) extent that this process can be parametrized in terms of c_s^2/Ω, the present analysis would still apply. We speculate that the stability of this point is actually significant, and that it is relevant for the experimentally observed stability of the strong central flux bundles in numerical simulations of accretion onto black holes.

4. CONCLUSIONS

We have considered the possibility that the angular momentum of an accretion disk is removed predominantly by outflows driven by the accreted field (Bisnovatyi-Kogan & Ruzmaikin 1974, Blandford 1976). An obstacle to this proposal has been the realization (van Ballegooijen 1989, Lubow et al. (1994)) that outward diffusions of the accreted field is fast compared to the inward accretion velocity in a geometrically thin accretion disk if the value of the Prandtl number P_m is around unity. Revisiting this problem, we find that even moderately weak fields can in fact cause sufficient angular momentum loss via a magnetic wind to balance outward diffusion. The estimate in Eq. (21) shows that, at $P_m = 1$, a field with a magnetic pressure as low as $\sim 10^{-3}$ of the gas pressure p_c at the disk midplane has a chance of facilitating its own accretion by driving a moderately strong magnetic outflow. This is due more or less to compounding numerical factors of order unity. In particular when MRI turbulence produces the relatively low effective viscosity $\alpha \sim 0.01$ that is seen in several numerical simulations.

Using a simplified model for the vertical disk structure, we have studied the conditions for existence of such stationary equilibria between wind-induced advection and outward turbulent diffusion in more quantitative detail. Two equilibrium points are found, one at low field strengths corresponding to a plasma-beta at the midplane of order several hundred, and one for strong accreted fields, $\beta \sim 1$. We surmise that the first is relevant for the accretion of weak, possibly external, fields through the outer parts of the disk, while the latter one could explain the tendency, observed in full 3D numerical simulations, of strong flux bundles at the centers of disk to stay confined in spite of strong MRI turbulence surrounding them (e.g. Beckwith et al. 2009). These authors also identify the mechanism responsible for maintenance of the bundle against the outward diffusion that one might expect from the turbulence surrounding it. Unlike the present model, this mechanism does not depend on the presence of a wind.

HS thanks the Shanghai Astronomical Observatory for their generous hospitality during the work on the project reported here. This work is supported by the National Basic Research Program of China (grant 2009CB824800), the NSFC (grants 11173043, 11121062 and 11233006), and the CAS/SAFEA International Partnership Program for Creative Research Teams (KJCX2-YW-T23).

REFERENCES

Anderson, J. M., Li, Z.-Y., Krasnopolsky, R., & Blandford, R. D. 2005, ApJ, 630, 945
Beckwith, K., Hawley, J. F., & Krolik, J. H. 2009, ApJ, 707, 428
Bisnovatyi-Kogan, G. S., & Ruzmaikin, A. A. 1974, Ap&SS, 28, 45
Bisnovatyi-Kogan, G. S., & Ruzmaikin, A. A. 1976, Ap&SS, 42, 401
Blandford, R. D. 1976, MNRAS, 176, 465
Blandford, R. D., & Payne, D. G. 1982, MNRAS, 199, 883
Cao, X. 2011, ApJ, 737, 94
Cao, X., & Spruit, H. C. 1994, A&A, 287, 80
Cao, X., & Spruit, H. C. 2002, A&A, 385, 289 (CS02)
Fromang, S., Papaloizou, J., Lesur, G., & Heinemann, T. 2009, Numerical Modeling of Space Plasma Flows: ASTRONUM-2008, 406, 9
Fromang, S., & Stone, J. M. 2009, A&A, 507, 19
Guan, X., & Gammie, C. F. 2009, ApJ, 697, 1901
Guilet, J., & Ogilvie, G. I. 2012a, MNRAS, 424, 2097
Guilet, J., & Ogilvie, G. I. 2012b, arXiv:1212.0855
Igumenshchev, I. V., Narayan, R., & Abramowicz, M. A. 2003, ApJ, 592, 1042
Kippenhahn, R., & Schlüter, A. 1957, ZAp, 43, 36
Konigl, A., & Pudritz, R. E. 2000, Protostars and Planets IV, 759
Lesur, G., & Longaretti, P.-Y. 2009, A&A, 504, 309
Lubow, S. H., Papaloizou, J. C. B., & Pringle, J. E. 1994, MNRAS, 267, 235
Lubow, S. H., Papaloizou, J. C. B., & Pringle, J. E. 1994, MNRAS, 268, 1010
Mestel, L. 2012, *Stellar magnetism*, second edition. Oxford science publications (International series of monographs on physics 154)
Narayan, R., & Yi, I. 1994, ApJ, 428, L13
Narayan, R., & Yi, I. 1995, ApJ, 452, 710
Ogilvie, G. I., & Livio, M. 2001, ApJ, 553, 158
Parker, E. N. 1979, in Chapter 17, Cosmical Magnetic Fields (Oxford:Clarendon Press)
Pudritz, R. E., Ouyed, R., Fendt, C., & Brandenburg, A. 2007, Protostars and Planets V, 277
Spruit, H. C. 1996, NATO ASIC Proc. 477: Evolutionary Processes in Binary Stars, 249
Spruit, H. C. 2010, Lecture Notes in Physics, Berlin Springer Verlag, 794, 233
Spruit, H. C., Stehle, R., & Papaloizou, J. C. B. 1995, MNRAS, 275, 1223
Spruit, H. C., & Uzdensky, D. A. 2005, ApJ, 629, 960
Stehle, R., & Spruit, H. C. 2001, MNRAS, 323, 587
van Ballegooijen, A. A. 1989, Accretion Disks and Magnetic Fields in Astrophysics, 156, 99
Yousef, T. A., Brandenburg, A., Rüdiger, G. 2003, A&A, 411, 321